Main Manuscript for

Enteric Populations of *Escherichia coli* are Likely to be Resistant to Phages Due to O Antigen Production

Brandon A. Berryhill[1,2], Kylie B. Burke[1,3], Jake Fontaine[1, †], Catherine E. Brink [4,5], Mason G. Harvill[1], David A. Goldberg[1], Konstantinos T. Konstantinidis [4,5], Bruce R. Levin[1], Michael H. Woodworth[3, *]

[1] Department of Biology, Emory University; Atlanta, Georgia, 30322, USA

[2] Program in Microbiology and Molecular Genetics (MMG), Graduate Division of Biological and Biomedical Sciences (GDBBS), Laney Graduate School, EmoryUniversity; Atlanta, Georgia, 30322, USA

[3] Division of Infectious Diseases, Department of Medicine, Emory University School of Medicine; Atlanta, Georgia, 30322, USA

[4] Ocean Science & Engineering, School of Biological Sciences, Georgia Institute of Technology, Atlanta, GA, USA

[5] School of Civil & Environmental Engineering, Georgia Institute of Technology, Atlanta, GA, USA

[†] Present Address: Graduate School of Arts and Sciences, Yale University, New Haven, Connecticut, 06520, USA

*Corresponding Author: Michael H. Woodworth

Email: michael.holmes.woodworth@emory.edu

Competing Interest Statement: The authors have no competing interests to declare.

Classification: Biological Sciences- Microbiology

Keywords: *Escherichia coli*, Bacteriophage, Population Biology, Phage Resistance, Fecal Microbiota Transplantation, O antigens, Enteric Microbiome

This PDF file includes:

Main Text
Figures 1 to 5
Tables 1

Abstract

Bioinformatic and experimental data show that bacteriophages are ubiquitous in human enteric microbiomes. However, there are gaps in understanding the contribution of these viruses in shaping the bacterial strain and species composition of the gut microbiome and how these phages are maintained over time. To address these questions, we adapted and analyzed the properties of a mathematical model of the population and evolutionary dynamics of bacteria and phage and performed experiments with *Escherichia coli* and phages isolated from four fecal

microbiota transplantation (FMT) doses as representative samples of non-dysbiotic enteric microbiota. Our models predict and experiments confirm that due to production of the O antigen, *E. coli* in the enteric microbiome are likely to be resistant to infection with co-occurring phages. However, phages can be maintained in these populations in high densities due to high rates of transition between resistant and sensitive states, which we call leaky resistance. Based on these models and observations, we postulate that the phages found in the human gut are likely to play little role in shaping the composition of *E. coli* in the enteric microbiome in healthy individuals. How general this is for other species of bacteria in enteric microbiota is not yet clear, although O antigen production is broadly conserved across many taxa.

Significance Statement

Little is known about the role that bacteriophages play in shaping the bacterial species and strain composition in the human gut microbiome or how they are maintained over time in this dynamic environment. Here we show that *Escherichia coli* isolated from fecal samples are likely to be resistant to their co-existing phages due to production of the O antigen. However, phages can be maintained in populations of mostly resistant bacteria if there is a rapid transition between resistant and sensitive states, a state called leaky resistance. Based on these results, we postulate that bacteriophages are likely playing little role of shaping the abundance and diversity of bacteria in the human gut microbiome in healthy individuals.

Main Text

Introduction

Within the last decade, research on the composition and function of the human microbiome has increased exponentially (1). The human microbiome is composed of trillions of microbes, including bacteria, viruses, fungi, protozoa, and archaea, that are found within and upon our bodies (2). The enteric (gut) microbiome, in particular, has been tightly linked to human health and well-being (3-5). Many of the greatest threats to human health such as cardiovascular disease, response to cancer chemotherapies, malnutrition, and antimicrobial resistance have also been linked to the gut microbiome (6-12). Interventions modifying the enteric microbiome could address many of these issues. However, realizing this much-anticipated therapeutic potential will require improved understanding of the microbial interactions that impact health and disease.

Most studies of the human gut microbiome employ culture-independent, bioinformatic approaches (13, 14). These bioinformatic-based studies infer “who is there” and suggest “what they are doing” from sequence data. While they are powerful and high-throughput approaches that have substantially advanced understanding of microbial communities, mechanistic studies to understand microbial competition (i.e. “who is infecting whom”) as an approach to modify the composition of species and strains in a given microbiome are best advanced with complementary methods (15). Understanding these interactive processes is critical to elucidating the mechanisms by which interventions may increase desirable and decrease less desirable microbiome functions.

One intervention that has shown clinical success in modifying microbiome states is fecal microbiota transplantation (FMT). FMT is performed by enteric administration of intestinal microbiota from a healthy donor, typically in a recipient with a microbiome-associated disease. The most frequent clinical use of FMT is prevention of recurrent *Clostridioides difficile* infection (RCDI) (16). Early-stage clinical trials have shown FMTs to also be highly efficacious at reducing colonization with multi-drug resistant bacterial organisms (MDRO) other than *C. difficile* (17-19). It has recently been shown that in addition to reducing the abundance of antibiotic resistant bacteria colonizing the enteric microbiome, FMTs may reduce recurrent MDRO infections (20). Beyond

clinical use, FMT has also become an important model of microbial ecology and microbial competition within the context of human hosts. However, the mechanisms by which FMT may modify the microbiome of recipients have just begun to be uncovered and the extent to which bacterial interactions fully account for the observed effects is unclear.

Metagenomic and limited experimental data suggest that the viral fraction of the enteric microbiota could contribute to the efficacy of FMT. For example, a small clinical trial with five patients receiving sterile filtrates of a donor's microbiome was shown to be as effective as FMT (21), with other studies finding qualitatively similar results (22). Similarly, a study of fecal filtrate transfer in a piglet model prevented necrotizing enterocolitis (23). Could bacteriophage (phage), a filterable element of the gut microbiome, be responsible for changing the composition and structure of the recipient's microbiome? Stated another way, could treating with an FMT be a kind of phage therapy? To address this question and understand the role phages may have in shaping species and strain compositions when transferred, we investigate the role of phages in determining the densities and distributions of *E. coli* strains within the gut microbiome of four individual healthy hosts who have qualified as FMT donors (20) using bioinformatics, mathematical models, and culture-based infection assays. We focused on *E. coli* due to its ubiquity in the human gut microbiome and because its phages have relatively large host ranges, unlike the phages of other enteric residents such as *Bacteroides spp (24).*

Results

E. coli and phage isolation from FMT doses

We first sought to isolate and characterize both major and minor populations of *E. coli* as well as the dominant *E. coli* bacteriophage populations from four FMT donors using the methods illustrated in Figure 1. We were not able to recover any bacteriophage via direct plating. Instead, to obtainphage, all FMT samples required the addition of both Lysogeny Broth (LB) and a broadly phage sensitive, non-lysogeny laboratory *E. coli* strain which lacks restriction modification enzyme

systems.phage sensitive, non-lysogeny laboratory *E. coli* strain which lacks restriction modification enzyme systems.

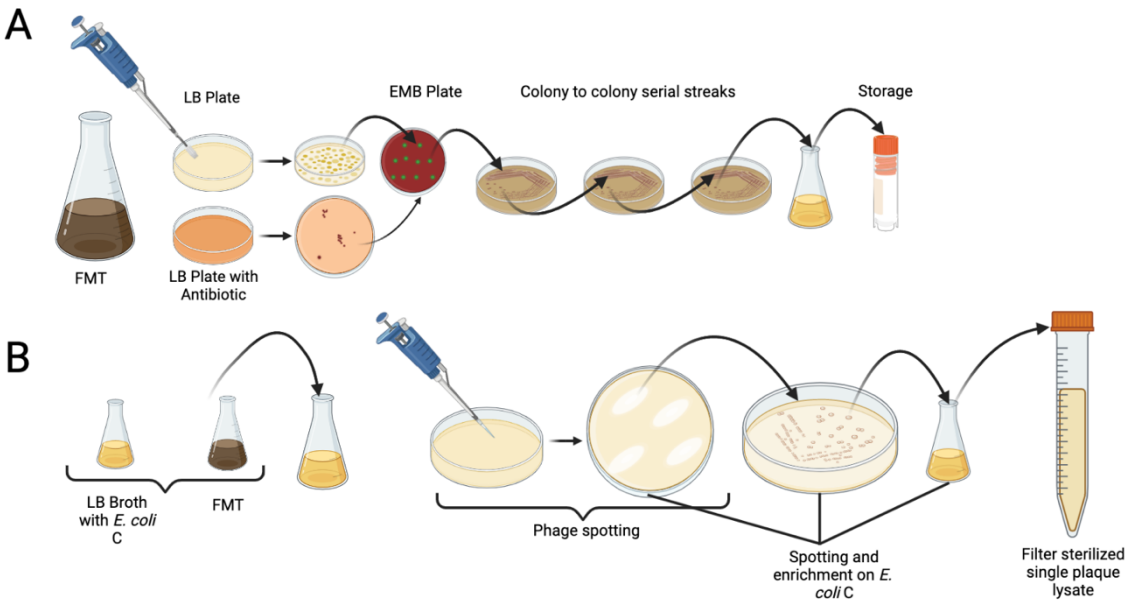

Figure 1. Diagram of bacteria and phage isolation protocol. (A) Method employed for isolating the dominant as well as minority populations of *E. coli* from the FMT samples. **(B)** Method employed for isolating bacteriophage from the FMT samples.

With selective culture methods and comparative genomic analysis, we identified an apparent dominant strain (representing more than half of all *E. coli* isolated from a sample) and several minority strains of *E. coli* in each sample as shown in Figure 2. For each FMT donor, we assessed the diversity of recovered *E. coli* strains by alignment of predicted gene clusters, average nucleotide identity (ANI), *in silico* multi-locus sequence type (MLST), and *in silico* H and O serotype prediction. When applying an ANI-based genomovar definition of conspecific isolates with ≥99.5% ANI, we identified a median of 2.5 (range 2-3) *E. coli* genomovars per donor (25). In general, classification by MLST was consistent with the ANI-based strain clustering. However, genomovars with high ANI and of the same MLST displayed greater diversity in predicted O antigen type. These findings show that healthy individuals carry diverse *E. coli* strains.

We also were able to recover three phages from three of the four donors, of note we were not able to recover any phages that formed plaques from Donor A. Phylogenetic analysis of the phage genomes were conducted by generating an average amino acid identity (AAI) heatmap (Supplemental Figure 1) and consensus maximum likelihood phylogenetic trees based on the core phage genomes (Figure 2 Panel B). Based on AAI, we see a clear segregation between the *Peduovirus* genomes and those of the lambda and T-phages, which make up most of the genomes in the other two major clusters in the heatmap. The *Peduovirus* genomes, genomes of this study, and the IMG/VR genomes shared AAI values of ≥90%, which reflects the high similarity in gene content between these genomes and provides support for placing the query genomes in this genus. The consensus tree of these gene trees, estimated using Astral (26), is shown in Figure 2 Panel B. The tree was rooted using *Escherichia virus vB_eco_mar005P1*. The additional two genomes as the outgroup were added manually to the tree, as these genomes shared too few genes with the *Peduovirus* genomes to construct a reliable phylogeny. Genomes

S12-S14 appear to be most closely related to *Escherichia virus P2-2H4* and *Enterobacteria phage fiAA91-ss* while genomes S6-S11 are more closely related to *Bacteriophage R18C* and *Yersinia phage vB YpM22* and *YpM50*. The phylogeny also shows that the genomes of donor D are only distantly related to those of B and C. The phages from donors B and C also appear to cluster separately, with the exception of S10, which is closely related to the genomes of donor B despite being isolated from donor C. This suggests that each donor has distinct phage populations.

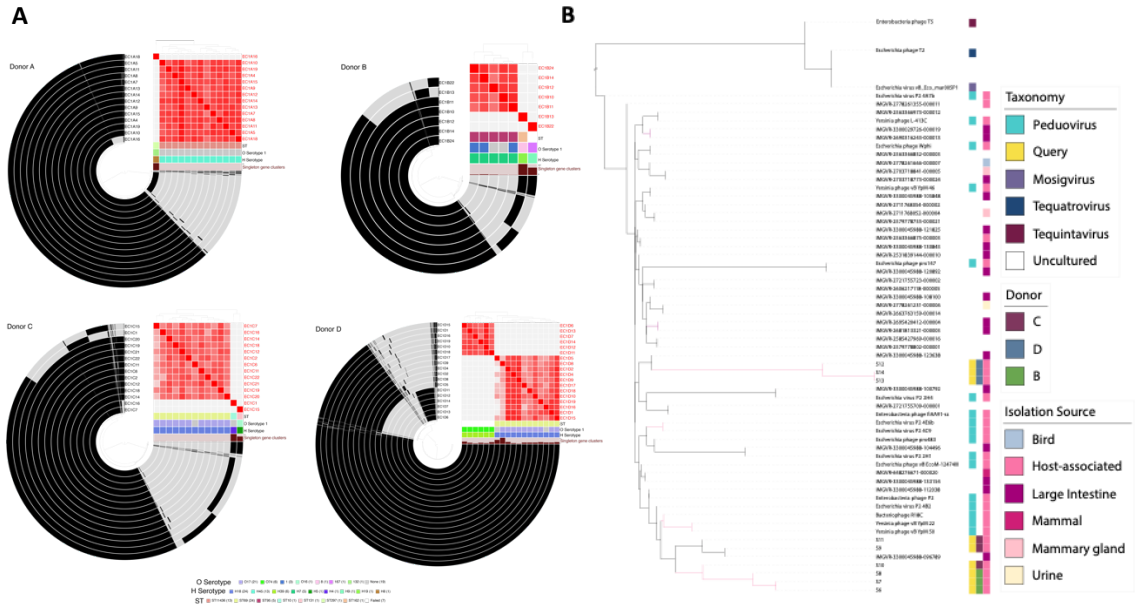

Figure 2. Diversity of isolated *E. coli* and phages. (A) Circular clustered gene alignments of *E. coli* isolated from four healthy donors show maintenance of minority populations that differ by average nucleotide identity (ANI, shown as red heat map scaled from 0.995 to 1.0), gene content (with singleton gene clusters ranging from 0 to 722), *in silico* multi-locus sequence type (MLST) classification, and *in silico* predicted O and H antigens. **(B)** Consensus Maximum Likelihood phylogenetic tree based on core genes of the genomes in this study and close relatives from public databases**.** Thirty-two genes were shared in more than 55/60 of the genomes in the major amino acid identity (AAI) cluster of Supplemental Figure 1 and were used to build individual trees as described in the Methods Section.

Susceptibility of *E. coli* isolates to phage

For bacteriophages to shape the composition of an established enteric microbiota, a substantial fraction of the resident *E. coli* must be sensitive to those phages. Therefore, we tested the susceptibility of the *E. coli* isolated above by spotting three classes of phages on lawns of each of the bacteria: i) well-characterized laboratory phages, ii) the co-existing phages isolated from the same donor, and iii) phages isolated from the other donors. In total, we tested 751 combinations of 54 bacterial isolates and 14 phage isolates. The laboratory strains of phages are expected to form clear plaques on lawns of sensitive bacteria. We find with the *E. coli* C lab strain that this is the case as all 14 tested lab and FMT-derived phage isolates produced clear plaques. As shown in Figure 3, this is not the case with the FMT-derived *E. coli* isolates, which give either no plaques (217/265, 81.9%) or turbid plaques (42/265, 15.8%) to the lab phages with one exception (T3 phage

spotted on EC1D8; 1/265, 0.3%). When spotting FMT-derived phages on FMT-derived *E. coli* isolates, 392/477 (82.2%) combinations produced no plaques and 85/477 (17.8%) produced turbid plaques.

For phages in FMT doses to shape the composition of a recipient's enteric microbiota, the recipient's *E. coli* must be sensitive to FMT-derived phage. However, when comparing combinations of FMT-derived phage and *E. coli* isolated from the same (autologous, e.g. phage from Donor B and *E. coli* from Donor B) or different donors (allogeneic, e.g. phage from Donor B and *E. coli* from Donor D) we do not find sensitivity. We found a significantly higher proportion of turbid plaques with autologous phage-*E. coli* combinations compared to allogeneic phage-*E. coli* combinations (29/117, 24.5% vs 56/360, 15.6%; chi-square p-value 0.033). Further analysis of these and the above pairs of bacteria and phage are described in Supplemental Table 2.

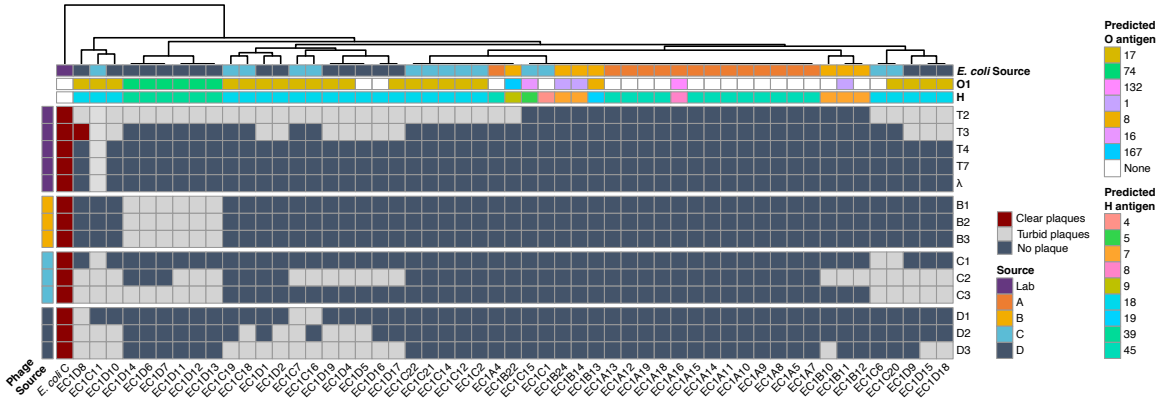

Figure 3. FMT isolated *E. coli* do not give clear plaques when spotted with laboratory or FMT-derived bacteriophages. Well-characterized laboratory and FMT-derived *E. coli* strains (Indicated by Source as Lab or A through D) were spotted with well-characterized laboratory (T2, T3, T4, T7, and a virulent mutant of phage λ) and FMT-derived bacteriophages (isolated from FMT donors B through D). Dark blue denotes no plaque formation, light grey denotes turbid plaque formation, and red denotes clear plaque formation. Clear plaques were only produced by the tested phages on lawns of a laboratory strain of *E. coli* C indicating broad resistance or immunity of FMT-derived *E. coli* to FMT-derived phages.

The O antigen as a mechanism for broad phage resistance

We hypothesized that the broad level of phage resistance found in the wild *E. coli* isolated from FMT doses may be explained by the display of the O antigen (27-29). This hypothesis is consistent with the fact that we can only isolate phage from the FMT samples by adding in both rich media and a broadly phage-sensitive lab strain of *E. coli*. Most lab strains, including *E. coli* C, do not produce the O antigen, while it is nearly ubiquitous among wild *E. coli*. As evidence in support of this O antigen hypothesis, we performed spot assays with MG1655 (an O antigen negative lab strain), MG1655L5 (a mutant of MG1655 expressing a medium level of the O antigen), MG1655L9 (a mutant of MG1655 strongly expressing the O antigen), and with the lab phage T7. MG1655L9 does not produce plaques as seen with many of the strains above in Figure 3. Importantly, lawns of MG1655L5 do produce plaques, but these plaques are turbid as in many of the cases seen above. We have restricted the assays with our constructed O antigen strains to the phage T7 as this phage is known to have its receptor masked via steric inhibition by the production and display of the O antigen, requires two mutations to resistance making the evolution of resistance unlikely

in our assays (30), and was shown in Figure 3 to form no plaques on all but one of the FMT isolated *E. coli*, though the plaques found on the exceptional isolate were turbid.

As additional evidence in support of the hypothesis that the O antigen is the reason for the broad level of phage resistance observed in human intestinal microbiota, we repeated the phage isolation protocol described in Figure 1B using MG1655 and both of the above O antigen construct, MG1655L5 and MG1655L9. Unlike MG1655, neither of these O antigen expressing strains were able to enrich the phages present in the fecal samples.

O antigen profile of enteric *E. coli*

We postulated that production of the O antigen could account for the lack of clear plaques observed in Figure 3. To ascertain if *E. coli* isolated from FMT doses bear the O antigen, we used the tool ECTyper to predict the O antigen type for each isolate (31). As shown in Table 1, we then experimentally confirmed O antigen production by antiserum agglutination assay for strains that were annotated by this tool. While our tool did not annotate the O antigen type of all of our isolated strains, we are confident that they are all O antigen positive based on the results of the spot assay (Figure 3).

Table 1. O antigen type and production of the FMT-derived *E. coli* isolates.

Strain	Predicted O antigen Type	Serology Confirmation
EC1A16	132	Positive
EC1B11	1	Negative
EC1B13	8	Positive
EC1B14	1	Positive
EC1B22	167	Positive
EC1B24	1	Positive
EC1C2	17/44	Positive
EC1C7	17/77	Positive
EC1C11	17/77/44	Positive
EC1C12	17/77	Positive
EC1C14	17/44	Positive
EC1C15	16	Positive
EC1C19	17/44	Positive
EC1C20	17/44	Positive
EC1C21	17/44	Positive
EC1C22	17/44	Positive
EC1C16	17/44	Positive
EC1C18	17/44	Positive
EC1D1	17/77	Positive
EC1D2	17/77/44	Positive
EC1D4	17/77/44	Positive
EC1D6	74	Positive
EC1D7	74	Positive
EC1D8	17/77	Positive
EC1D9	17/77	Positive
EC1D12	74	Positive
EC1D13	74	Positive
EC1D14	74	Positive
EC1D15	17/44	Positive
EC1D17	17/44	Positive

EC1D18	17/77/44	Positive
EC1D19	17/77	Positive
EC1D10	17/77	Positive
EC1D11	74	Positive

If the bacteria are resistant, how are the phage still present in the enteric microbiome?

Despite the observed resistance, we are still able to isolate bacteriophages from these FMT doses. How are these phages maintained if the dominant population is resistant? We postulated that phage maintenance may occur due to what has been called Leaky Resistance, where there is a high transition rate from a resistant state to a sensitive state, providing a sufficient density of sensitive cells on which the phage can replicate. For this analysis, we adapted our model from Chaudhry et al. (32). In Supplemental Figure 2, we present a diagram of our mathematical model of the population and evolutionary dynamics of lytic phage and bacteria. In the Supplemental Text, Supplemental Equations, and Supplemental Table 1, we detail two mathematical models and their parameters that could account for the presence of lytic and free temperate phages in the FMTs which are dominated by resistance. The results of the model with temperate phages (Supplemental Figure 3) are qualitatively similar to that with the lytic phage.

The predictions of this model and a parallel experiment are presented in Figure 4 and Figure 5, respectively.

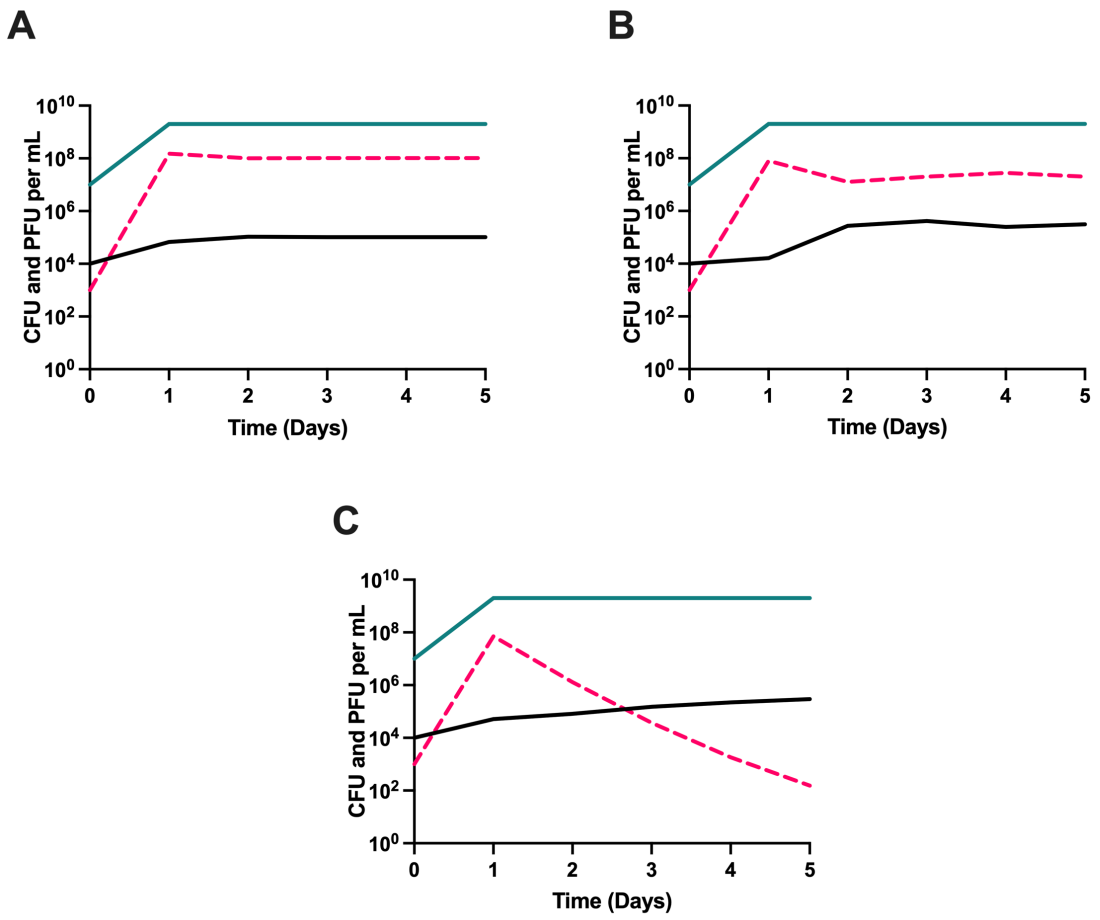

Figure 4. Predicted serial transfer dynamics of O antigen mediated resistance and a lytic phage. Simulation results, changes in the initial and end of transfer densities of bacteria and phage in serial transfer culture with three different transition rates between states. Where 1000µg/ml of the limiting resource is added at each transfer. **A-** Transition rates from sensitive to resistant and from resistant to sensitive of 10^{-5} per cell per hour. **B-** Transition rates from sensitive to resistant and from resistant to sensitive of 10^{-4} per cell per hour, and **C-** Transition rates from sensitive to resistant and from resistant to sensitive of 10^{-3} per hour. O antigen expressing cells- turquoise, Sensitive cells-black, Phage – pink.

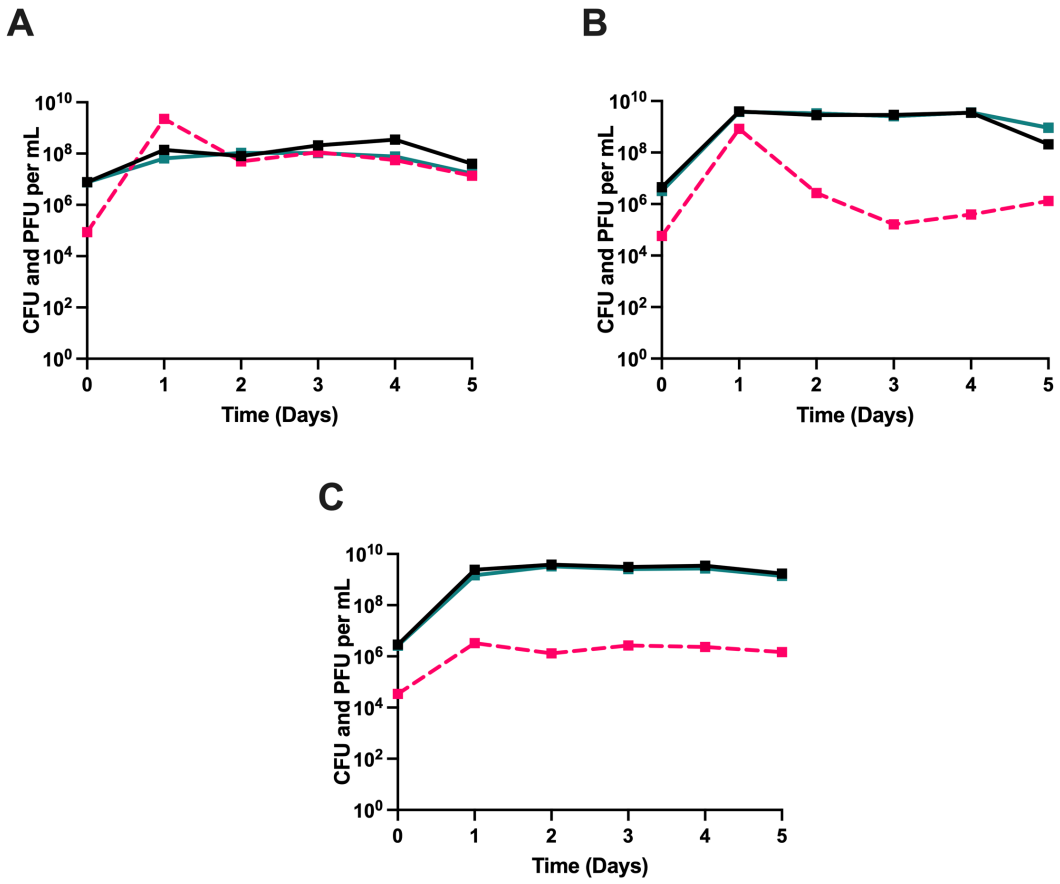

Figure 5. Serial transfer of T7 with MG1655 lacking and expressing the O antigen. Three variants of *E. coli* MG1655 serially transferred for five days in LB broth with the phage T7. Shown in solid lines are bacterial densities with the black line representing a phage free control. The broken lines present phage densities. Each color is one of three biological replicates. **(A)** Wild type MG1655 not expressing the O antigen. **(B)** MG1655L5 expressing a medium amount of the O antigen. **(C)** MG1655L9 expressing a high amount of the O antigen.

The mathematical model predicts that for the phage to be maintained on minor populations of sensitive cells, the transition rate between resistant and sensitive must be in excess of 10^{-5}. Although we are unable to estimate the density of sensitive cells in our experiments, we find with MG1655, MG1655L5, and MG1655L9 that the phage are maintained, albeit at different levels. This is consistent with the mutation rate to sensitivity being at least 10^{-5} and demonstrates that Leaky Resistance could account for how the phage are maintained in wild isolates from human intestinal microbiota despite the bacterial population being dominated by resistance.

Evolution of O antigen mediated phage resistance

Critical to the evolution of a novel phenotype is the ability of the genes encoding that phenotype to increase when rare. Presumably the *E. coli* colonizing humans use the O antigen to protect against phagocytosis. This is one probable reason that naturally occurring *E. coli* bear and express the genes for the O antigen. The results of this study suggest there is an additional selective force for the evolution of the O antigen: bacteriophage predation. Consistent with this hypothesis is the observation that *in vitro* O antigen expressing bacteria increase in frequency when rare in a population of O antigen deficient cells when bacteriophage are present (Supplemental Figure 4).

Discussion

We set out to elucidate the role of bacteriophages in determining the densities of and shaping the strain and species composition of bacteria in the enteric microbiome. Our primary interpretation of these results is that in the microbiome of healthy individuals, bacteriophages play little role in determining the density, strain, and species composition of the bacteria in the enteric microbiome due to the high prevalence of phage resistance. In the case of *E. coli*, this resistance is a consequence of the production of the O antigen. Moreover, we expect that this same O antigen-mediated resistance phenomenon will manifest in all Enterobacteriaceae. Stated another way, we postulate that resistance to co-occurring phages will be the dominant characteristic of bacteria in stable natural communities. This prediction is consistent with experimental studies of lytic and temperate bacteriophages *in vitro* (30, 33).

Resistant mutants almost always emerge and ascend to become the dominant population of bacteria in *in vitro* experiments with laboratory strains of bacteria and lytic phages. Nevertheless, phages are commonly maintained in these cultured populations that are dominated by resistant bacteria. We expected to observe some degree of specificity of phage and O antigen serotype plaquing. However, despite testing 477 combinations, we did not detect clear phage-serotype clustering among these wild isolates. Production of O antigen, more than O antigen type, appeared to be the most strongly associated with resistance in this study. There are a variety of mechanisms by which the phage can be maintained, but their maintenance appears to play little role in regulating the densities of these cultures and these populations are more likely shaped by other selective pressures such as resource availability. We postulate this is also the case in the gut microbiome, although additional work with clinical specimens that reflect in situ states could extend the laboratory work presented here. There is, however, a caveat to our purported mechanism for phage maintenance in that one prediction of our model is that the density of bacteria would exceed that of phage in natural populations. How common that is in natural communities is unclear as in marine settings it is thought that the density of phage far exceeds that of the bacteria (34, 35), though recent studies have questioned how high this ratio actually is (36).

We expect that the approach elaborated in this study also has broader utility for translational phage investigation. If phages are to be developed as therapeutics or as adjunctive components of live biotherapeutic product consortia, we expect that this will require complementary culture-based and culture-independent techniques that include experimental isolation, characterization, and strain-resolved analysis in the context of complex communities. We expect O antigen production to account for resistance of *E. coli* to co-occurring phage in the intestinal microbiota of healthy individuals at steady state. However, these findings do not discount the possibility that phages contribute to FMT efficacy in other ways such as indirect effects on other bacterial taxa that permit or restrict colonization with Enterobacterales or host immunomodulatory effects.

Fueled by the increasing incidence of antibiotic resistant infections in recent years there has been a resurrection of interest in using bacteriophage to treat bacterial infections. When it comes to utilizing bacteriophages therapeutically, one would expect a tradeoff between this generalized

resistance mechanism and virulence. This phenomenon was illustrated in classical work by Smith and Huggins, where they utilized a phage targeting the K antigen of pathogenic *E. coli (37)*. Interestingly, the mechanism of resistance explored here, the O antigen, is known to be the target of some bacteriophages. If the results presented here for *E. coli* are at all general, we would expect difficulties in isolating phage capable of lysing specific bacterial isolates. This anticipated result is echoed by investigators working on isolating phage for therapy where the rates of finding phage for an isolate are less than 50% for some pathogens (38, 39). Here we provide one explanation for why this is the case, resistance associated with production of the O antigen.

Materials and Methods

Bacterial Strains. *E. coli* C was obtained from Marie-Agnès Petit at INRAE in Joy-en-Josas, France. MG1655 L9 and L5 were obtained from Douglas Browning at Aston University in Birmingham, UK. Wild *E. coli* were isolated from fecal microbiota transplantation doses as described below.

Bacteriophages. Phages Lambda^{VIR}, T2, T3, T4, and T7 were acquired from the Levin Lab's phage collection. Wild phages were isolated from fecal microbiota transplantation doses as described below.

Growth Media and Conditions. Unless otherwise noted, all bacteria were cultured in Lysogeny Broth (LB) at 37 °C. Lysogeny broth (LB) prepared according to manufacturer instructions (Difco, REF# 244620). LB soft agar made with 0.7% w/v agarose, and LB plates made with 1.6% agarose, LB phage plates prepared as LB plates supplemented with 20 mM $CaCl_2$.

Isolating Bacteria from the FMTs. Serial dilutions of FMT in 0.85% NaCl solution was followed by plating on Davis Minimal (DM) plates (Sigma-Aldrich, 15758) supplemented with 0.4% w/v lactose (Sigma-Aldrich, L3750). Individual colonies were randomly chosen and picked with a sterile stick and simultaneously streaked onto an EMB plate and a DM plate. Both were incubated at 37 °C overnight. Isolates colored green on the EMB plate were picked from their its respective minimal plate and serially streaked from the DM lactose plate onto another DM lactose plate and incubated at 37 °C overnight. Each isolate was labeled, stored, and frozen.

Isolating Phage from the FMTs. 0.1 mL of FMT suspension was inoculated into 10mL LB broth with ~1e^7 CFU/mL *E. coli* C. These flasks were grown with shaking at 37 °C overnight. The next day, samples were centrifuged and filtered through a 0.22-micron filter (Basix, 13-1001-06). These rough lysates were then plated for single plaques. Individual plaques were picked with a sterile stick and resuspended as described above to obtain clonal phage lysates.

AAI heatmap. We identified the closest relatives to the genomes of this study (query genomes) using whole-genome searches against public genome databases. The final set of genomes used in subsequent analyses consisted of 98 genomes – including the 9 query genomes, 34 genomes from the IMG/VR v4 database (40), and 55 genomes that are publicly available on NCBI. Prodigal v2.6.3 (41) was used for gene prediction with default settings, and pairwise all versus all Average Amino acid Identity (AAI) was calculated using the aai.rb script from the Enveomics collection (42) using default settings except for decreasing the number of minimum hits to 20. The final heatmap was constructed using the pheatmap package in R. Accession numbers of the public genomes are labelled in the figure.

Core gene tree. The subset of genomes that make up the major cluster in the AAI heatmap were used for gene clustering at 30% identity with MMseqs2 v 13.4511 (43). The resulting clusters were used to identify the core genome – the genes that are found in 55/60 (~90%) of the genomes. The 32 core genes were extracted using seqtk-1.4 and individual gene alignments were generated using MUSCLE v3.8.31 (44) with default settings. Each alignment was used to generate a maximum likelihood gene tree in MEGA11 (44) with default parameters. These gene

trees were concatenated and passed into Astral 5.7.8 (26) to generate the final consensus tree as Astral has a built-in algorithm to deal with any missing data in the input gene trees. The final tree was visualized and annotated in iTol (45) and is shown in Figure 2B.

Phage Susceptibility Testing. ~$1e^4$ of each phage lysate was spotted onto lawns of the bacteria using the double-layer soft agar technique as described in (46).

Sampling Bacterial and Phage Densities. Bacteria and phage densities were estimated by serial dilutions in 0.85% NaCl solution followed by plating. The total density of bacteria was estimated on LB (1.6%) agar plates. To estimate the densities of free phage, chloroform was added to suspensions before serial dilutions and double-layer soft agar enumeration.

Serial Transfer Experiments. All serial transfer experiments were carried out in 10 mL LB broth cultures grown at 37 °C with vigorous shaking. The cultures were initiated by 1:100 dilution from 10 mL overnight cultures grown from single colonies. Phage was added to these cultures to reach the initial density of~10^7 PFU/mL. At the end of each transfer, 0.1 mL of each culture was transferred into flasks with fresh medium (1:100 dilution). Simultaneously,0.1 mL samples were taken for estimating the densities of CFUs and PFUs as described above.

Antibiotics and Their Sources. Streptomycin (S6501) was obtained from Sigma-Aldrich; Tetracycline (T1700) from Research Products International; Gentamicin (BP918-1) from Fisher BioReagents; Chloramphenicol (C5793) from Sigma-Aldrich; Ciprofloxacin (A4556) from AppliChem); Ceftriaxone (C5793) from Sigma-Aldrich; Meropenem (QH-8889) from Combi-Blocks; Azithromycin (3771) from Tocris; Fosfomycin (P5396) from Sigma-Aldrich; and Colistin (C4461) from Sigma-Aldrich. All antibiotic Sensi-Discs were obtained from Becton Dickinson.

O Antigen Antisera Assay. *E. coli* O antigen specific antisera was obtained from SSI Diagnostica and used as detailed in their protocol for the slide agglutination assay. A known O antigen negative lab strain (MG1655) and its construct bearing the O antigen (MG1655L9) were used as negative and positive controls respectively.

Whole-Genome Sequencing. Samples were sent to MIGS (Pittsburgh, USA) as bacterial colonies grown on an agar plate or as sterile phage lysates for extraction and Illumina sequencing. Individual colonies and lysates were extracted per the manufacturer's protocol using Zymo's DNA miniprep bead beating lysis kit. Sample libraries were prepared for Illumina sequencing using Illumina's DNA Prep kit and IDT 10bp unique dual indices and sequenced on an Illumina NovaSeq 6000, producing paired end 151bp reads. Demultiplexing, quality control, and adapter trimming was performed with bcl-convert (v4.1.5). Illumina reads were quality filtered using Trimmomatic (47). *E. coli* C host sequences were depleted from phage lysate sequencing data by mapping to a closed *E. coli* C genome with bowtie2 (48). After trimming and host decontamination (for phage lysates), remaining reads were and assembled *de novo* using SPAdes v3.13 (49). Pairwise comparisons of average nucleotide identity on the assembled genomes were performed with the Mashmap method using fastANI v1.32 as in (50). Gene sequences were predicted with Prodigal v2.6.3 (41) and annotated with Prokka v1.14.6 (51). O and H antigens were predicted *in silico* with ECtyper (31). Bacterial pangenome figures were created with anvi'o v.7.1 (52).

Numerical Solutions (Simulations). For our numerical analysis of the coupled, ordered differential equations presented (Supplemental Equations 1-8) we used Berkeley Madonna using the parameters presented in Supplemental Table 1. Copies of the Berkeley Madonna programs used for these simulations are available at www.eclf.net.

Statistical Analysis. Statistical tests of difference in proportions of phage plaquing results tabulated as a contingency table were performed with the chisq.test function in stats package

version 4.3.0 in R version 4.3.0 using the R studio interface version 2023.06.0. Resulting p-values <0.05 were considered statistically significant.

Acknowledgments:

We thank Dalia Gulick, Amanda Strudwick, Amalia Cruz, and Candace Miller for their help obtaining and processing the FMTs. We also thank the other members of the Levin Lab for their collaboration and discussion in particular Andrew Smith, Josh Manuel, Teresa Gil-Gil, Thomas O'Rourke, Ingrid McCall, and Eduardo Roman. We would like to thank BioRender for their software which was used to create the schematic figure.

Funding Sources
National Institute of Allergy and Infectious Diseases grant K23AI144036 (MHW)
Southern Society for Clinical Investigation Research Scholar Award (MHW)
National Institute of General Medical Sciences grant R35GM136407 (BRL)
The content is solely the responsibility of the authors and does not necessarily represent the official views of the National Institutes of Health or the Southern Society for Clinical Investigation.

Data Availability
The Berkeley Madonna program used for the simulations are available at ECLF.net. All raw sequence data for the *E. coli* and phage genomes shown have been deposited in the sequence read archive (SRA, NCBI, Bethesda, MD, USA) and can be found with bioproject accession PRJNA1028583.

References

1. L. Proctor *et al.*, A review of 10 years of human microbiome research activities at the US National Institutes of Health, Fiscal Years 2007-2016. *Microbiome* **7**, 31 (2019).
2. M. Matijašić *et al.*, Gut Microbiota beyond Bacteria-Mycobiome, Virome, Archaeome, and Eukaryotic Parasites in IBD. *Int J Mol Sci* **21** (2020).
3. G. A. Ogunrinola, J. O. Oyewale, O. O. Oshamika, G. I. Olasehinde, The Human Microbiome and Its Impacts on Health. *Int J Microbiol* **2020**, 8045646 (2020).
4. K. Hou *et al.*, Microbiota in health and diseases. *Signal Transduction and Targeted Therapy* **7**, 135 (2022).
5. T. Wilmanski *et al.*, Gut microbiome pattern reflects healthy ageing and predicts survival in humans. *Nature Metabolism* **3**, 274-286 (2021).
6. D. Davar *et al.*, Fecal microbiota transplant overcomes resistance to anti–PD-1 therapy in melanoma patients. *Science* **371**, 595-602 (2021).
7. W. Zhu *et al.*, Gut Microbial Metabolite TMAO Enhances Platelet Hyperreactivity and Thrombosis Risk. *Cell* **165**, 111-124 (2016).
8. K. H. Liu *et al.*, Microbial metabolite delta-valerobetaine is a diet-dependent obesogen. *Nat Metab* **3**, 1694-1705 (2021).
9. M. H. Woodworth, M. K. Hayden, V. B. Young, J. H. Kwon, The Role of Fecal Microbiota Transplantation in Reducing Intestinal Colonization With Antibiotic-Resistant Organisms: The Current Landscape and Future Directions. *Open Forum Infect Dis* **6** (2019).
10. S. Tomkovich *et al.*, Human colon mucosal biofilms from healthy or colon cancer hosts are carcinogenic. *J Clin Invest* **129**, 1699-1712 (2019).
11. C. E. DeStefano Shields *et al.*, Reduction of Murine Colon Tumorigenesis Driven by Enterotoxigenic Bacteroides fragilis Using Cefoxitin Treatment. *J Infect Dis* **214**, 122-129 (2016).
12. M. I. Smith *et al.*, Gut microbiomes of Malawian twin pairs discordant for kwashiorkor. *Science* **339**, 548-554 (2013).
13. B. Gao *et al.*, An Introduction to Next Generation Sequencing Bioinformatic Analysis in Gut Microbiome Studies. *Biomolecules* **11**, 530 (2021).
14. R. Knight *et al.*, Best practices for analysing microbiomes. *Nature Reviews Microbiology* **16**, 410-422 (2018).
15. J. Puschhof, E. Elinav, Human microbiome research: Growing pains and future promises. *PLOS Biology* **21**, e3002053 (2023).
16. W. Jung Lee, L. D. Lattimer, S. Stephen, M. L. Borum, D. B. Doman, Fecal Microbiota Transplantation: A Review of Emerging Indications Beyond Relapsing Clostridium difficile Toxin Colitis. *Gastroenterol Hepatol (N Y)* **11**, 24-32 (2015).

17. G. Battipaglia *et al.*, Fecal microbiota transplantation before or after allogeneic hematopoietic transplantation in patients with hematologic malignancies carrying multidrug-resistance bacteria. *Haematologica* **104**, 1682-1688 (2019).

18. J. Bilinski *et al.*, Fecal Microbiota Transplantation in Patients With Blood Disorders Inhibits Gut Colonization With Antibiotic-Resistant Bacteria: Results of a Prospective, Single-Center Study. *Clin Infect Dis* **65**, 364-370 (2017).

19. D. B. Steed *et al.*, Gram-Negative Taxa and Antimicrobial Susceptibility after Fecal Microbiota Transplantation for Recurrent Clostridioides difficile Infection. *mSphere* **5**, e00853-00820 (2020).

20. M. H. Woodworth *et al.*, Fecal microbiota transplantation promotes reduction of antimicrobial resistance by strain replacement. *Sci Transl Med* **15**, eabo2750 (2023).

21. S. J. Ott *et al.*, Efficacy of Sterile Fecal Filtrate Transfer for Treating Patients With Clostridium difficile Infection. *Gastroenterology* **152**, 799-811.e797 (2017).

22. A. Brunse *et al.*, Fecal filtrate transplantation protects against necrotizing enterocolitis. *The ISME Journal* **16**, 686-694 (2022).

23. Y. Hui *et al.*, Donor-dependent fecal microbiota transplantation efficacy against necrotizing enterocolitis in preterm pigs. *NPJ Biofilms Microbiomes* **8**, 48 (2022).

24. A. J. Hryckowian *et al.*, Bacteroides thetaiotaomicron-Infecting Bacteriophage Isolates Inform Sequence-Based Host Range Predictions. *Cell Host Microbe* **28**, 371-379.e375 (2020).

25. L. M. Rodriguez-R *et al.*, A natural definition for a bacterial strain and clonal complex. *bioRxiv* 10.1101/2022.06.27.497766, 2022.2006.2027.497766 (2022).

26. S. Mirarab *et al.*, ASTRAL: genome-scale coalescent-based species tree estimation. *Bioinformatics* **30**, i541-i548 (2014).

27. A. K. Golomidova *et al.*, O antigen restricts lysogenization of non-O157 Escherichia coli strains by Stx-converting bacteriophage phi24B. *Sci Rep* **11**, 3035 (2021).

28. Y. A. Knirel *et al.*, Variations in O-Antigen Biosynthesis and O-Acetylation Associated with Altered Phage Sensitivity in Escherichia coli 4s. *Journal of Bacteriology* **197**, 905-912 (2015).

29. P. van der Ley, P. de Graaff, J. Tommassen, Shielding of Escherichia coli outer membrane proteins as receptors for bacteriophages and colicins by O-antigenic chains of lipopolysaccharide. *J Bacteriol* **168**, 449-451 (1986).

30. L. Chao, B. R. Levin, F. M. Stewart, A Complex Community in a Simple Habitat: An Experimental Study with Bacteria and Phage. *Ecology* **58**, 369-378 (1977).

31. K. Bessonov *et al.*, ECTyper: in silico Escherichia coli serotype and species prediction from raw and assembled whole-genome sequence data. *Microb Genom* **7** (2021).

32. W. N. Chaudhry *et al.*, Leaky resistance and the conditions for the existence of lytic bacteriophage. *PLoS Biol* **16**, e2005971 (2018).

33. B. A. Berryhill *et al.*, The book of Lambda does not tell us that naturally occurring lysogens of Escherichia coli are likely to be resistant as well as immune. *Proceedings of the National Academy of Sciences* **120**, e2212121120 (2023).

34. J. H. Paul, M. B. Sullivan, A. M. Segall, F. Rohwer, Marine phage genomics. *Comparative Biochemistry and Physiology Part B: Biochemistry and Molecular Biology* **133**, 463-476 (2002).

35. S. Chibani-Chennoufi, A. Bruttin, M. L. Dillmann, H. Brüssow, Phage-host interaction: an ecological perspective. *J Bacteriol* **186**, 3677-3686 (2004).

36. S. Roux, J. R. Brum, Counting dots or counting reads? Complementary approaches to estimate virus-to-microbe ratios. *The ISME Journal* **17**, 1521-1522 (2023).

37. H. W. Smith, M. B. Huggins, Successful treatment of experimental Escherichia coli infections in mice using phage: its general superiority over antibiotics. *J Gen Microbiol* **128**, 307-318 (1982).

38. S. Mattila, P. Ruotsalainen, M. Jalasvuori, On-Demand Isolation of Bacteriophages Against Drug-Resistant Bacteria for Personalized Phage Therapy. *Front Microbiol* **6**, 1271 (2015).

39. S. Aslam *et al.*, Lessons Learned From the First 10 Consecutive Cases of Intravenous Bacteriophage Therapy to Treat Multidrug-Resistant Bacterial Infections at a Single Center in the United States. *Open Forum Infectious Diseases* **7** (2020).

40. A. P. Camargo *et al.*, IMG/VR v4: an expanded database of uncultivated virus genomes within a framework of extensive functional, taxonomic, and ecological metadata. *Nucleic Acids Research* **51**, D733-D743 (2022).

41. D. Hyatt *et al.*, Prodigal: prokaryotic gene recognition and translation initiation site identification. *BMC Bioinformatics* **11**, 119 (2010).

42. L. M. Rodriguez-R, K. T. Konstantinidis, The enveomics collection: a toolbox for specialized analyses of microbial genomes and metagenomes. *PeerJ Preprints* **4**, e1900v1901 (2016).

43. M. Steinegger, J. Söding, MMseqs2 enables sensitive protein sequence searching for the analysis of massive data sets. *Nature Biotechnology* **35**, 1026-1028 (2017).

44. K. Tamura, G. Stecher, S. Kumar, MEGA11: Molecular Evolutionary Genetics Analysis Version 11. *Molecular Biology and Evolution* **38**, 3022-3027 (2021).

45. I. Letunic, P. Bork, Interactive Tree Of Life (iTOL) v5: an online tool for phylogenetic tree display and annotation. *Nucleic Acids Research* **49**, W293-W296 (2021).

46. A. M. Kropinski, A. Mazzocco, T. E. Waddell, E. Lingohr, R. P. Johnson, Enumeration of bacteriophages by double agar overlay plaque assay. *Methods Mol Biol* **501**, 69-76 (2009).

47. A. M. Bolger, M. Lohse, B. Usadel, Trimmomatic: a flexible trimmer for Illumina sequence data. *Bioinformatics* **30**, 2114-2120 (2014).

48. B. Langmead, S. L. Salzberg, Fast gapped-read alignment with Bowtie 2. *Nat Methods* **9**, 357-359 (2012).

49. A. Prjibelski, D. Antipov, D. Meleshko, A. Lapidus, A. Korobeynikov, Using SPAdes De Novo Assembler. *Curr Protoc Bioinformatics* **70**, e102 (2020).

50. C. Jain, L. M. Rodriguez-R, A. M. Phillippy, K. T. Konstantinidis, S. Aluru, High throughput ANI analysis of 90K prokaryotic genomes reveals clear species boundaries. *Nature Communications* **9**, 5114 (2018).

51. T. Seemann, Prokka: rapid prokaryotic genome annotation. *Bioinformatics* **30**, 2068-2069 (2014).

52. A. M. Eren *et al.*, Community-led, integrated, reproducible multi-omics with anvi'o. *Nat Microbiol* **6**, 3-6 (2021).

Supporting Information for

O Antigen Mediated Bacteriophage Resistance in Enteric *Escherichia coli* Populations

Brandon A. Berryhill, Kylie B. Burke, Jake Fontaine, Catherine E. Brink, Mason G. Harvill, David A. Goldberg, Konstantinos T. Konstantinidis, Bruce R. Levin, Michael H. Woodworth

Supplemental Text

In the following, we use a mathematical-computer simulation model to illustrate how populations dominated by phage-resistant, O antigen-bearing bacteria will maintain populations of lytic and temperate phages.

Model of the population dynamics of resistant O antigen bearing bacteria and lytic phage

There are two populations of bacteria, one bears an O antigen, O, that masks the phage receptor, and the other is a variant of the O antigen-bearing bacteria, S, for which the receptor is available for the phage to adsorb. There is a single population of lytic phage, P. The variables O, S, and P are the designations of these populations and their densities, cells and particles per ml for the bacteria and phage, respectively.

The bacteria replicate at a rate proportional to their maximum growth rates, respectively v_O and v_S, and a hyperbolic function of the concentration of a limiting resource, r μg/ml. $\psi(r) = \frac{r}{(k+r)}$ where k is the resource concentration when the growth rate is half its maximum value, the Monod constant (1). For our analysis of the properties of this model, we use the same value of k for both O and S. The limiting resource is taken up at a rate proportional to the sum of the product of the densities of the populations, their maximum growth rates, the Monod function, ψ(r) and a conversion efficiency parameter, e μg per cell. The phage infects the bacteria at a rate equal to the product of the densities of bacteria and phage and rate parameter, δ_O and δ_S per ml, ml attacks per phage particle per cell per hour with, $\delta_O << \delta_S$. Each infected bacterium produces β phage particles. The O population transitions to S, and the S transition to O at a rate of μ_{OS} and μ_{SO} per cell per hour, respectively. To account for the decline in the physiological state of the bacteria as

the resource decline, we assume the rates of phage infection and transition between states are proportional to ψ(r) (2, 3).

With these definitions and assumptions, the rates of change in the concentration of the limiting resource and densities of the bacteria and phage are given by,

$$\frac{dr}{dt} = -\psi(r) \bullet e \bullet (v_O \bullet O + v_S \bullet S)$$

$$\frac{dO}{dt} = v_O \bullet O \bullet \psi(r) - \delta_O \bullet O \bullet P \bullet \psi(r) + (\mu_{SO} \bullet S - \mu_{OS} \bullet O) \bullet \psi(r)$$

$$\frac{dS}{dt} = v_S \bullet S \bullet \psi(r) - \delta_S \bullet S \bullet P \bullet \psi(r) + (\mu_{OS} \bullet S - \mu_{SO} \bullet O) \bullet \psi(r)$$

$$\frac{dP}{dt} = \delta_O \bullet O \bullet P \bullet \psi(r) \bullet \beta + \delta_S \bullet S \bullet P \bullet \psi(r) \bullet \beta$$

To solve these equations and those that follow for the temperate phage, we use Berkeley Madonna. In these numerical solutions, simulations, we assume the populations are maintained in serial transfer culture. Every 24 hours, the populations of bacteria and diluted by a factor of 1/100, and 1000μg/ml of fresh resource is added.

In Figure 4, we present the results of simulations with three rates of transition between O and S, μ_{OS} and μ_{SO} per cell per hour.

If the rate of transition between the sensitive, S, and resistant O antigen-bearing state is great enough, the phage is maintained in a population dominated by resistant O antigen-bearing bacteria. In the above simulations, we are assuming sensitive and resistant, S and O, bacteria have the same growth rate. The conditions for the maintenance of the phage would be greater if the O antigen mediated resistance had a fitness cost, $v_O < v_S$.

Model of the population dynamics of resistant O antigen bearing bacteria and temperate phage

There are two populations of lysogenic bacteria, one bearing the O antigen and one without the O antigen, with designations and densities OL and L, respectively. There is a single population of free temperate phage of density PT particles per ml. The phage can adsorb to L, with a rate constant δ, but cannot adsorb to the OL. Temperate phages that adsorb to lysogens are lost. With rates of ind_{OL} and ind_L, the OL and L lysogens are induced and produce β_{OL} and β_L phage particles, respectively, with the induced OL and L dying. As with the lytic phage model, we assume that all rates are proportional to the concentration of the limiting resource by a Monod function, $\psi(r) = \frac{r}{(r+k)}$, and the limiting resource is taken up at a rate proportional $\psi(r)$, their growth rates and densities, and a conversion efficiency parameter, e μg/per cell. We neglect the loss of the prophage by the OL and L lysogens.

With these definitions and assumptions, the rates of change in the densities of bacteria are given by,

$$\frac{dr}{dt} = -\psi(r) \bullet e \bullet (v_{OL} \bullet OL + v_L \bullet L)$$

$$\frac{dOL}{dt} = v_O \bullet OL \bullet \psi(r) - ind_{OL} \bullet OL \bullet \psi(r) + (\mu_{LOL} \bullet L - \mu_{OLL} \bullet OL) \bullet \psi(r)$$

$$\frac{dL}{dt} = v_L \bullet L \bullet \psi(r) - ind_L \bullet L \bullet \psi(r) + (\mu_{OLL} \bullet OL - \mu_{LOL} \bullet L) \bullet \psi(r)$$

$$\frac{dPT}{dt} = ind_{OL} \bullet OL \bullet \beta_{OL} \bullet \psi(r) + ind_L \bullet L \bullet \beta_L \bullet \psi(r) - \delta \bullet PT \bullet L \bullet \psi(r)$$

In Supplemental Figure 3, we present the results of simulations of the population dynamics of temperate phage and lysogens that mask the receptor and do not adsorb the phage, OL, and lysogens with the receptor open to adsorption by PT, L.

In all cases bacterial populations are dominated by “resistant”, O antigen bearing lysogens, substantial densities of free temperate phage are maintained.

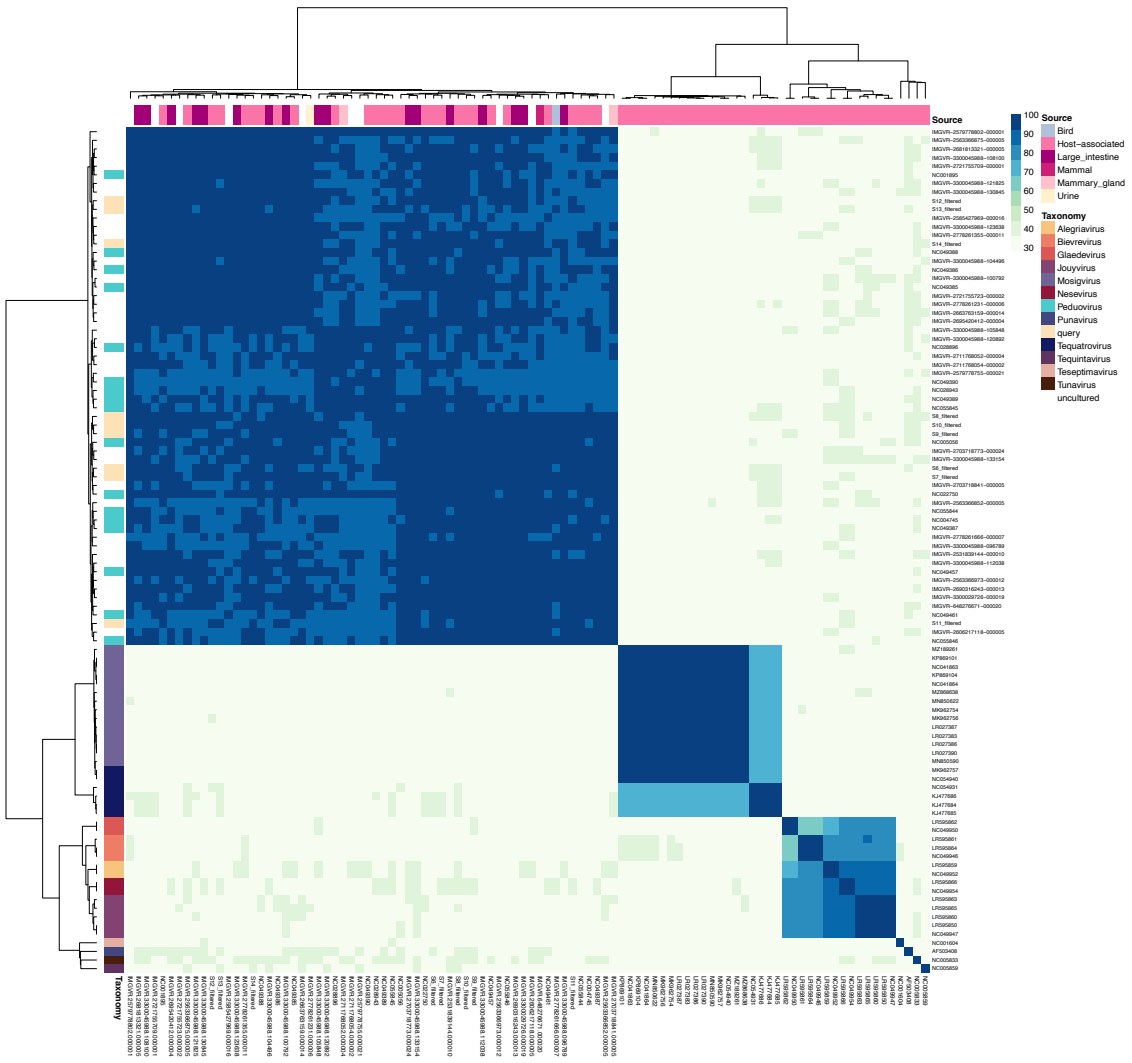

Figure S1. Heatmap of average amino acid identities (AAIs) among genomes of this study and selected reference genomes from public databases. AAI was estimated based on BLAST+ whole-genome comparisons using a minimum alignment identity of 20% and at least 20 genes shared between two genomes. Genomes of this study were clearly placed in the major AAI cluster that included all *Peduovirus* genomes from IMG/VR and several close relatives from

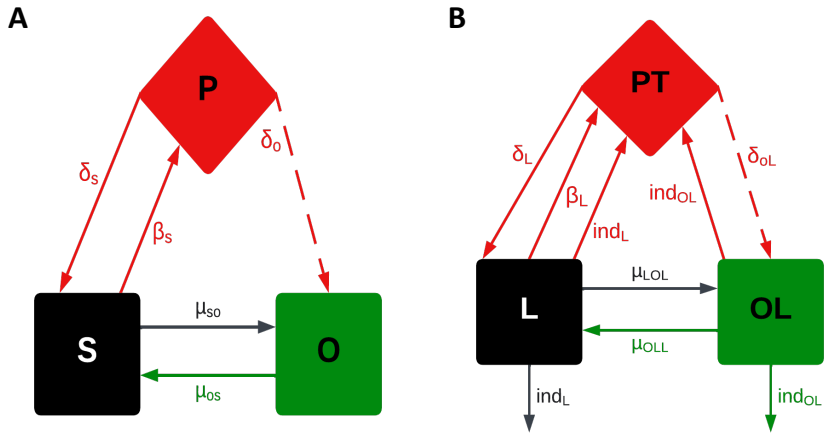

Figure S2. **Models of the population and evolutionary dynamics of O antigen mediated phage resistance.** See the supplemental text for a description of the model and Supplemental Table 1 for the definitions and dimensions of the parameters and the values used in our numerical solutions to the equations and simulations. **A)** There is a population of lytic phage, P; a population of phage-sensitive bacteria, S; and a population of phage-resistant, O antigen producing cells, O. **B)** There is a population of temperate phage, PT; a population of immune lysogens, L; and a population of phage-resistant, O antigen producing lysogens, OL.

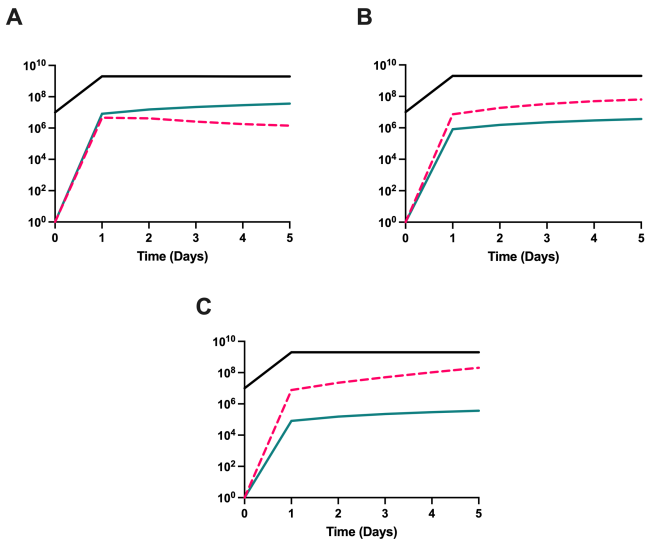

Figure S3. Predicted serial transfer dynamics of O antigen mediated resistance and a temperate phage. Simulation results, changes in the initial and end of transfer densities of bacteria and phage in serial transfer culture. 1000μg/ml of the limiting resource is added at each transfer. Standard parameters, $v_O = v_S = 2.0$ per cell per hour, $e = 5x10^{-7}$ μg/cell, k=1.0, β=50, $\delta_O=0$, $\delta_S – 2x10^{-7}$ per phage per cell per hour. **A-** $\mu_{OS}=\mu_{SO}=10^{-5}$ per cell per hour. **B-** $\mu_{OS}=\mu_{SO}=10^{-4}$ per cell per hour, and **C-** $\mu_{OS}=\mu_{SO}=10^{-3}$ per hour. O antigen expressing lysogenic cells- turquoise, Lysogenic cells-black, Phage – pink.

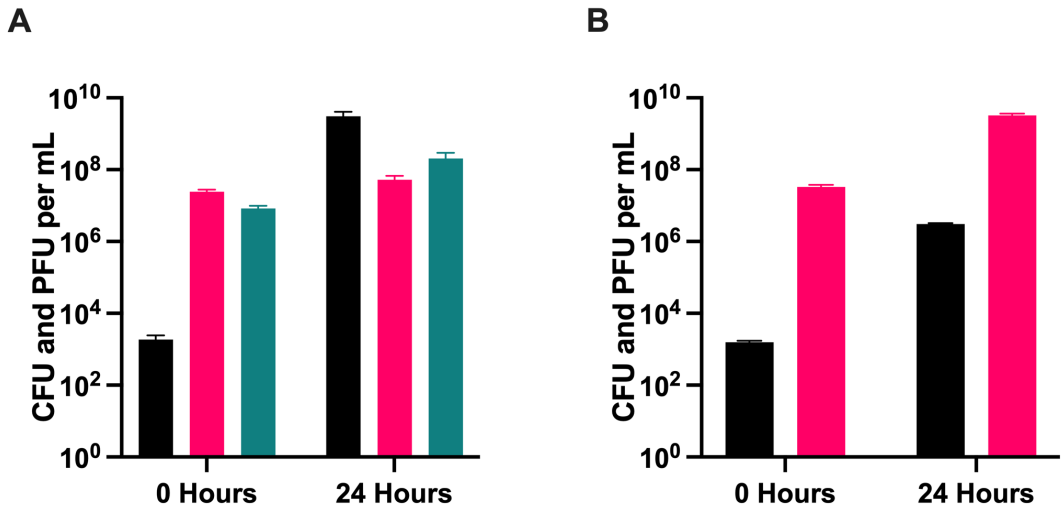

Figure S4. Invasion when rare experiment of O antigen expressing cells into a population of O antigen deficient cells. Shown are the results of an experiment initiated with **(A)** 10^3 O-antigen expressing cells, 10^7 O-antigen deficient cells, and 10^7 lytic phage or **(B)** 10^3 O-antigen expressing cells, 10^7 O-antigen deficient cells, and no phage. Shown are mean and standard deviations of three biological replicates. O antigen expressing cells are in black, O antigen

Table S1. Parameter definitions, units, and values used in generating the mathematical models and computer simulations.

Parameter	Value (dimensions)	Description	Source
v_O, v_S	2.0 (h^{-1})	Maximum growth rates	This paper
μ_{OS}, μ_{SO}	$1e^{-5}$, $1e^{-5}$, or $1e^{-4}$ (h^{-1})	Transitions O → S, S → O	Chaudhry 2018 (4)
δ_O, δ_S	$2e^{-7}$ (h^{-1}·mL^{-1})	Adsorption rate constants	Chaudhry 2018 (4)
β	60 (PFU·CFU^{-1})	Burst size	Berryhill 2023 (5)
λ	$1e^{-2}$	Probability of lysogeny	Berryhill 2023 (5)
ind	$1e^{-4}$ (h^{-1})	Induction rate	Berryhill 2023 (5)
k	1 (μg)	Monod constant	Stewart and Levin 1973 (3)
e	$5e^{-7}$ (μg·CFU^{-1})	Conversion efficiency	Stewart and Levin 1973 (3)

Table S2: Summary of lysate spotting experimental results.

	None (N=392)	Turbid (N=85)	P-value
FMT *E. coli* source			
Allogeneic	304 (77.6%)	56 (65.9%)	0.0334
Autologous	88 (22.4%)	29 (34.1%)	
O1			
17	143 (36.5%)	46 (54.1%)	<0.001
74	27 (6.9%)	27 (31.8%)	
132	9 (2.3%)	0 (0%)	
1	26 (6.6%)	1 (1.2%)	
8	9 (2.3%)	0 (0%)	
16	9 (2.3%)	0 (0%)	
167	9 (2.3%)	0 (0%)	

	None (N=392)	Turbid (N=85)	P-value
None predicted	160 (40.8%)	11 (12.9%)	
O2			
1	9 (2.3%)	0 (0%)	<0.001
16	9 (2.3%)	0 (0%)	
44	76 (19.4%)	14 (16.5%)	
74	14 (3.6%)	13 (15.3%)	
77	67 (17.1%)	32 (37.6%)	
132	9 (2.3%)	0 (0%)	
None predicted	208 (53.1%)	26 (30.6%)	
O3			
17	64 (16.3%)	17 (20.0%)	0.754
44	13 (3.3%)	5 (5.9%)	
None predicted	315 (80.4%)	63 (74.1%)	
O4			
44	10 (2.6%)	8 (9.4%)	0.0146
77	54 (13.8%)	9 (10.6%)	
None predicted	328 (83.7%)	68 (80.0%)	
H			
4	9 (2.3%)	0 (0%)	<0.001
5	9 (2.3%)	0 (0%)	
7	41 (10.5%)	4 (4.7%)	
8	9 (2.3%)	0 (0%)	
9	9 (2.3%)	0 (0%)	
18	162 (41.3%)	54 (63.5%)	
19	9 (2.3%)	0 (0%)	
39	27 (6.9%)	27 (31.8%)	
45	117 (29.8%)	0 (0%)	

SI References

1. J. Monod, THE GROWTH OF BACTERIAL CULTURES. *Annual Review of Microbiology* **3**, 371-394 (1949).

2. B. R. Levin, F. M. Stewart, L. Chao, Resource-Limited Growth, Competition, and Predation: A Model and Experimental Studies with Bacteria and Bacteriophage. *The American Naturalist* **111**, 3-24 (1977).

3. F. M. Stewart, B. R. Levin, Partitioning of Resources and the Outcome of Interspecific Competition: A Model and Some General Considerations. *The American Naturalist* **107**, 171 - 198 (1973).

4. W. N. Chaudhry *et al.*, Leaky resistance and the conditions for the existence of lytic bacteriophage. *PLoS Biol* **16**, e2005971 (2018).

5. B. A. Berryhill *et al.*, The book of Lambda does not tell us that naturally occurring lysogens of Escherichia coli are likely to be resistant as well as immune. *Proceedings of the National Academy of Sciences* **120**, e2212121120 (2023).